Elementary magnitude comparators and flip-flop using Si_3N_4 based microring resonator

ANKUR SAHARIA[a,*], NITESH MUDGAL[a], ANKIT AGARWAL[a], KAMAL KISHOR CHOURE[a,e], JALIL ALI[b], PREECHA YUPAPIN[c,d], RAVI KUMAR MADDILA[a], GHANSHYAM SINGH[a]
[a]*Department of Electronics and Communication Engineering, MNIT, Jaipur, India*
[b]*Laser Centre, IBNU SINA ISIR, Universiti Teknologi Malaysia 81310 Johor Bahru, Malaysia*
[c]*Computational Optics Research Group, Advanced Institute of Materials Science, Ton Duc Thang University, Vietnam*
[d]*Faculty of Applied Sciences, Ton Duc Thang University, District 7, Ho Chi Minh City, Vietnam*
[e]*Department of ECE, Poornima Institute of Engineering & Technology, Jaipur, India*

This article present a unique approach for the implementation of all-optical magnitude comparators and J-K flip-flop. In this paper we have presented a numerical analysis of Si_3N_4 based optical microring resonator. The Si_3N_4 based microring resonator is modulated using optical pump signal. In this article we have utilised the nonlinear properties of silicon nitride to obtain the switching of signal and the theoretical study is proved using simulation results. We have also obtained the various figures of merit like on-off ratio, extinction ratio, quality factor and finesse which proves the practical feasibility of the proposed structure.

(Received August 6, 2019; accepted February 17, 2020)

Keywords: Microring resonator, Resonant wavelength, Logic circuit, Silicon nitride

1. Introduction

The current era is a generation of fast computing and all-optical logic gates provide the platform for the generation high-speed computation circuits and ultra-fast processing units. The optical computation gives enormous benefits over normal electronics components e.g. immune to electronic interference, smaller size and higher bandwidth. The logic gates/circuits using optical components has been discussed various times and many techniques have been utilized for the generation of all-optical logic circuits. The implementation of the various optical logic gate using photonic crystal was discussed in [1]. The logic gates designed with much better accuracy were explained using soliton conversion methods. [2-3]. Along with this many researchers have explained the construction of logic circuits using semiconductor optical amplifier [4]. The MMI based optical logic circuit based on BPSK modulation was explained in [5]. Lots of efforts were put in by various researches to explain combinational circuits [6] and sequential circuits [7] with the help of Mach Zehnder Interferometer. The importance of optical sequential cannot be ignored, the demonstration of all-optical sequential circuits using laser diodes [8] and using soliton conversion [9] was explained extensively. A method to obtain all-optical logic function using quantum dot was also explained by researchers [10]. These all-optical logic circuits and logic gates are basic bricks for the formation of high-speed processors and large optical networks. The logic circuits and basic logic gates utilizing micro-ring resonators [11-13] as a basic block have shown tremendous application and performance in integrated optics [14].

This paper gives a detailed description of the mathematical modelling of the ring resonator. In this paper we have described the construction of 1 bit, 2 bit magnitude comparators and J-K flip-flop using optical microring resonator. The ring resonators circuits are more suitable for monolithic integrated circuits fabrication and proposed device can be used effectively. We have utilised various combination of optical microring resonator to obtain the desired result. The paper has been structured in the following way section II comprised of mathematical analysis of the ring resonator and its switching operation based on nonlinearity, section III and IV includes the structure of 1 bit comparator using a combination of optical microring resonator and its result analysis, section V and VI contains 2 bit comparator and its simulation results, J-K flip-flop and its analysis are described in section VIII and IX followed by conclusion acknowledgement and biblography.

2. Mathematical analysis and operation principle

The primary structure of optical microring resonator includes one directional coupling between bus waveguides and a ring cavity shown in Fig. 1. The ring resonator has four-port structure Input, Through, Add and Drop as shown. We have used nonlinear material Si_3N_4 for our structure due to its higher bandgap energy. This material has the linear refractive index of 1.98 and non-linear

refractive index of 2.4×10^{-15}cm^2/W. The fraction (α_1, the coupling coefficient of input coupling region) of the incoming signal has been transmitted to the ring waveguide in the "on resonance" state of the ring, in this state the constructive interference occurs and length of an optical path of the signal is the multiple of effective length. The drop port received the maximum output in "on resonance" stage as the α_2 (coupling coefficient between output bus waveguide and the ring) couples the signal in this port. On the other hand, through port received the minimum signal in this state. A logic switch can be produced with this working ring resonator if we use non-linear material of the construction of ring resonator. Through the vertical pumping of the signal (as shown in Fig. 2) in the ring resonator, the extra electron-hole pair can be generated. These charge carrier due to non-linearity of the material causes a shift in the refractive index and hence change the resonant wavelength of the ring resonator. Thus the shift in wavelength can be used to turn the signal in "on" and "off" state at a particular output port of the microring resonator.

If we assume the radius of the ring cavity is R then the circumference of the ring also called the length of the ring can be given by L = 2πR, α_1 and α_2 are the coupling coefficient among the input-output waveguides and ring cavity respectively. The attenuation constant of the cavity given by "a", wave propagation constant is given by k_n where $k_n = \left(\frac{2\pi}{\lambda}\right).n_{eff}$ and λ is resonant wavelength of the cavity ($\lambda_{res} = \frac{2\pi R n_{eff}}{m}, m\ is\ integer$) and n_{eff} is the effective refractive index given by $n_{eff} = n_0 + n_2$ I, it can also be denoted by $n_{eff} = n_0 + (n_2.\mathrm{P}/A_{eff})$, where P and I are the power and the intensity of the pump signal and n_0, n_2 represent the linear and nonlinear indices of the material, A_{eff} is effective cross-sectional area, there is one factor called the intensity insertion loss coefficients denoted by γ.

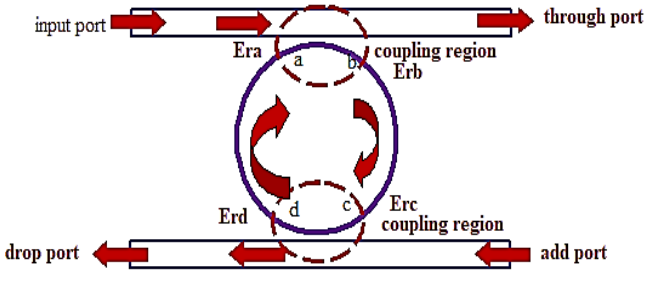

Fig. 1. Schematic of the ring resonator

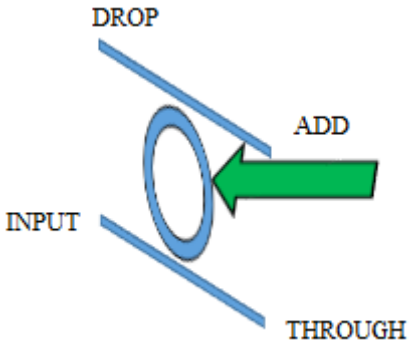

Fig. 2. Vertical pumping on ring resonator

Let us assume the incoming signal at the input port is $\boldsymbol{E_{i1}}$ and input signal at drop port is denoted by $\boldsymbol{E_{i2}}$. We also assuming electric field at four different points (a, b, c, d) are $\boldsymbol{E_{ra}}, \boldsymbol{E_{rb}}, \boldsymbol{E_{rc}}, \boldsymbol{E_{rd}}$ respectively and mathematically can be given by [15-17]

$$\boldsymbol{E_{ra}} = (1-\gamma)^{1/2}[j\sqrt{\alpha_1}.\boldsymbol{E_{i1}} + \sqrt{1-\alpha_1}.\boldsymbol{E_{rd}}] \quad (1)$$

$$\boldsymbol{E_{rb}} = \boldsymbol{E_{ra}}.\exp\left(-\frac{a.L}{4}\right).\exp(jk_n.\frac{L}{2}) \quad (2)$$

$$\boldsymbol{E_{rc}} = (1-\gamma)^{1/2}[j\sqrt{\alpha_2}.\boldsymbol{E_{i2}} + \sqrt{1-\alpha_2}.\boldsymbol{E_{rb}}] \quad (3)$$

$$\boldsymbol{E_{rd}} = \boldsymbol{E_{rc}}.\exp\left(-\frac{a.L}{4}\right).\exp(jk_n.\frac{L}{2}) \quad (4)$$

Therefore the electric field relation for the through port and drop port can be further denoted by [15]

$$\boldsymbol{E_t} = (1-\gamma)^{1/2}[j\sqrt{\alpha_i}.\boldsymbol{E_{rd}} + \sqrt{1-\alpha_1}.\boldsymbol{E_{i1}}] \quad (5)$$

$$\boldsymbol{E_d} = (1-\gamma)^{1/2}[j\sqrt{\alpha_2}.\boldsymbol{E_{rb}} + \sqrt{1-\alpha_2}.\boldsymbol{E_{i2}}] \quad (6)$$

If we further resolve the equations from (1) to (6) the propagating fields at both the ports wiz. through and the drop can be represented in the following form [16-17].

$$\boldsymbol{E_t} = \frac{\boldsymbol{D}(\sqrt{1-\alpha_1})-\boldsymbol{D}\sqrt{(1-\alpha_2)}\boldsymbol{x^2exp^2(j\phi)}}{1-\sqrt{1-\alpha_1}\sqrt{(1-\alpha_2)}\boldsymbol{x^2exp^2(j\phi)}}.\boldsymbol{E_{i1}} + \frac{-\boldsymbol{D}\sqrt{(\alpha_1)}\sqrt{(\alpha_2)}\boldsymbol{xexp(j\phi)}}{1-\sqrt{1-\alpha_1}\sqrt{(1-\alpha_2)}\boldsymbol{x^2exp^2(j\phi)}}.\boldsymbol{E_{i2}} \quad (7)$$

$$\boldsymbol{E_d} = \frac{\boldsymbol{D}(\sqrt{1-\alpha_1})-\boldsymbol{D}\sqrt{(1-\alpha_2)}\boldsymbol{x^2exp^2(j\phi)}}{1-\sqrt{1-\alpha_1}\sqrt{(1-\alpha_2)}\boldsymbol{x^2exp^2(j\phi)}}.\boldsymbol{E_{i2}} + \frac{-\boldsymbol{D}\sqrt{(\alpha_1)}\sqrt{(\alpha_2)}\boldsymbol{xexp(j\phi)}}{1-\sqrt{1-\alpha_1}\sqrt{(1-\alpha_2)}\boldsymbol{x^2exp^2(j\phi)}}.\boldsymbol{E_{i1}} \quad (8)$$

For simplification, we have assumed $D = (1-\gamma)^{1/2}$, $x = D.exp(-\frac{aL}{4})$ and $\phi = k_nL/2$. These equations are

vital for understanding the working of ring resonator for switching applications and also help to connect ring resonator in cascade for complex configuration. For a single stage of ring resonator if we kept $\boldsymbol{E_{i2}} = 0$ the output optical intensities of both the ports through and drop can be given by the following relations.

For further simplification assume $y_1 = \sqrt{(1-\alpha_1)}$ and $y_2 = \sqrt{(1-\alpha_2)}$

$$\frac{I_t}{I_{i1}}(\phi) = \left|\frac{E_t}{E_{i1}}\right|^2 = 1 - \frac{(1-y_1^2).(1-y_2^2x^2)}{(1-y_1y_2x)^2+4y_1y_2\,x\,sin^2(\frac{\phi}{2})} \quad (9)$$

$$\frac{I_d}{I_{i1}}(\phi) = \left|\frac{E_d}{E_{i1}}\right|^2 = \frac{(1-y_1^2).(1-y_2^2).x}{(1-y_1y_2x)^2+4y_1y_2\,x\,sin^2(\frac{\phi}{2})} \quad (10)$$

At resonance the through port have zero intensity ($k_nL = 2m\pi$) as the signal is completely extracted by the resonator. The minimum and maximum transmission is this state of the structure can be given as

For through port

$$T_{max} = \frac{(y_1+y_2x)^2}{(1+y_1y_2x)^2} \quad (11)$$

$$T_{min} = \frac{(y_1-y_2x)^2}{(1-y_1y_2x)^2} \quad (12)$$

For drop port

$$T_{max} = \frac{(1-y_1^2).(1-y_2^2).x}{(1-y_1y_2x)^2} \quad (13)$$

$$T_{min} = \frac{(1-y_1^2).(1-y_2^2).x}{(1+y_1y_2x)^2} \quad (14)$$

3. Design of 1 bit magnitude comparator

The design of 1 bit comparator is shown in Fig. 3. The layout of the design contains three microring resonators. The microring resonator 2 and 3 has been pumped with the optical pulse signal B and microring resonator 1 pumped with signal A. The through port of mrr3 will give the high output if bit A is less than B while the drop of mrr3 produce signal high if A is greater than B. On the other hand whenever A is equals to B the through port of mrr2 will produce the output high. The operation of microring resonator (mrr) will be same as explained in earlier section i.e. the ring is assumed to be resonate at the particular wavelength (ʎ), the input signal incident at input port will appear at drop port if there is no pumping or pumping pulse at logic low while input will appear at through port if pump pulse is at level high. The design parameters of ring resonators are shown in Table 1.

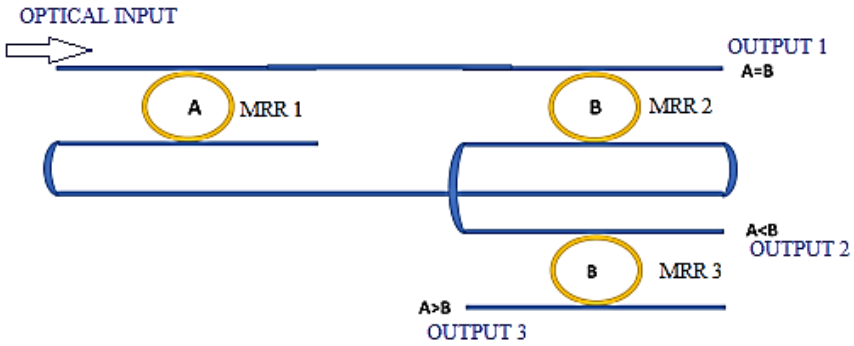

Fig. 3. Layout of 1 bit comparator

Table 1. Design parameters for ring resonator

S.N	Parameter	Value
1	Coupling coefficients (α_1 and α_2)	0.35
2	Resonance wavelength(ʎ)	1.55 µm
3	The radius of the ring (R)	20 µm
4	Intensity attenuation co-efficient of the ring(a)	0.0005 μm^{-1}
5	Coefficient of Intensity insertion loss (γ)	5%
6.	Ring width	900nm
7.	Bus waveguide length, width, height	100nm, 900nm, 644nm
8.	The gap between ring and bus waveguides	450 nm

4. Simulation analysis

The microring resonator is designed using Si_3N_4. The higher bandgap of silicon nitride and higher CMOS compatibility making it a suitable candidate for resonator design. The parameter considered for simulation purpose is shown in Table 1. We have kept the coupling coefficient 0.35 to improve the figure of merit for our design. The simulation output for 1-bit magnitude comparator is shown in Fig. 4. The figure is shown four combinations of 1-bit inputs. Column 1 and 2 represent two input bits A and B while column 3,4 and 5 represents the three outputs(A=B, A<B,A>B). The combination will produce respective outputs

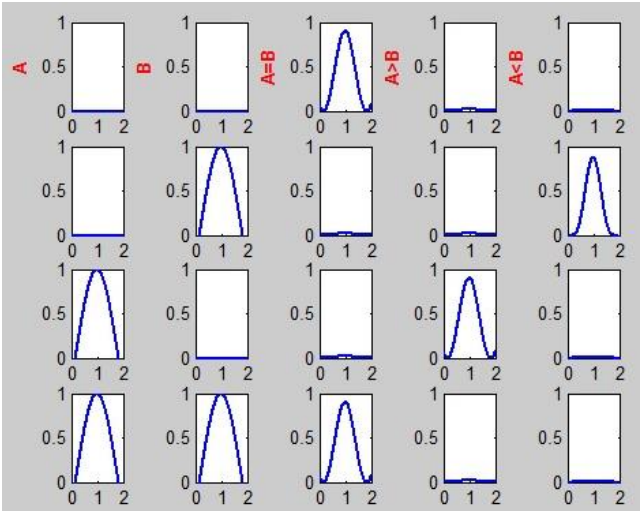

Fig. 4. Output of 1-bit comparator varying from A=00 to 11 and varying B from 00 to 11(color online)

Case I (A=0, B=0): In this case, the input of the more will be transferred to the through port of mrr 2. The absence of the pumping signal will make the ring resonate at the resonating frequency and produce output high at A=B.

Case II (A=0 and B=1): In this situation, the first resonator transferred the output at its drop port which acts as input for the second mrr and as the pumping pulse is high at second and third resonator the signal is transferred to their through ports. The output finally appeared at the output through port of third mrr (A<B).

Case III(A=1 and B=0): In this case the input signal is transferred to the drop port of mmr2 as the first resonator will be on resonance state while 2 and 3 mrr will be in off-resonance state. The input of mrr1 will finally appeared at the drop port of mrr3 which gives the output A>B.

Case IV (A=1, B=1): When both the pumping pulses are high the input is transferred to the through port of 1 and 2 resonators and produce A=B high.

5. Design of 2 bit comparator

The layout of 2 bit magnitude comparator is shown in Fig. 5. The implementation of the design includes 11 ring resonators. The microring resonators have been applied with 2 bit optical pulses A and B (A1A0, B1B0). The input is provided at the input port of mrr 1 and input port of mrr 6. The output A=B is taken from mrr 11. The output A>B is a combination of mrr7, mrr8 and mrr10. Similarly the third output A<B is taken as the combination of mrr4, mrr5 and mrr10.

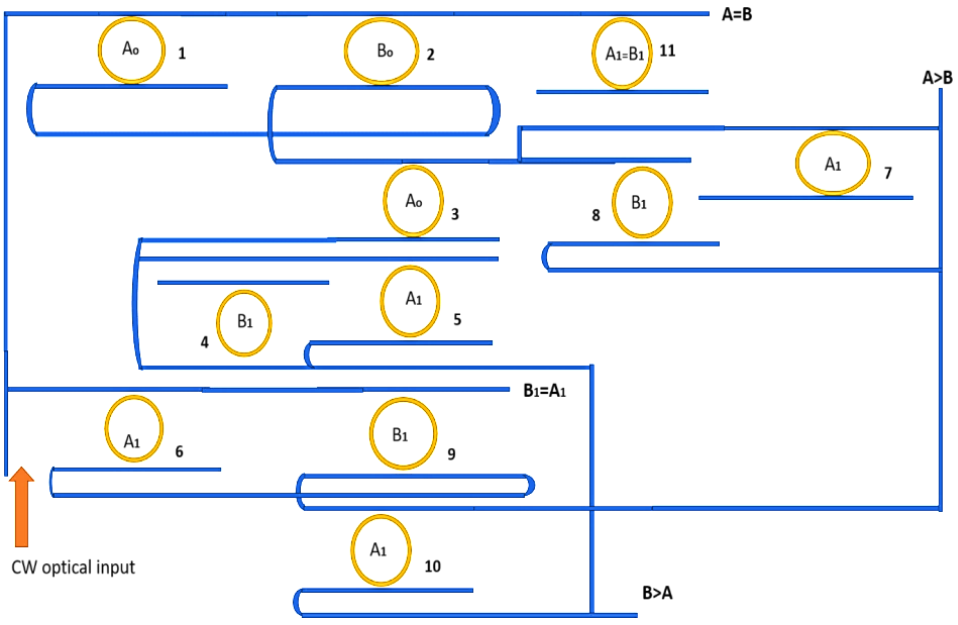

Fig. 5. Layout of 2 bit magnitude comparator

6. Simulation analysis

The layout of 2-bit comparator designed to given three different output at an instant. The output A=B is a combinational of mrr1, mrr2, mrr10 and mrr 11. The through port of mrr11 will give output A=B. Similarly, the through port of mrr7 will give the output A>B which is a combination of mrr7, 8 and 10. Similarly the drop port of mrr 5 gives A<B which is a combination of mrr4, mrr5 and mrr10. The outputs of 2 bit comparator is shown in Fig. 6-9. The first two columns showing the pump signal A(A1A0) and next two columns are showing pump pulse B(B1B0) rest three columns are showing outputs A=B, A<B, A>B. The different combinations of inputs for two-bit comparator are explained below.

Case 1 (A=00, B=00): In this case, as both the pump pulse are off, therefore, all the mrr's will be in on resonance state. The input is inserted at the input port of mrr1 and mrr 6. As the pump signal is at logic 0 therefore the signal is transferred to drop ports of both mrr, and then appeared at the through port of mrr2 and 9 respectively. These two outputs are taken as input and pump signal for mrr 11 since the pump is high therefore the through port of mrr11 will give the output A=B.

Case 2 (A=00, B=01): In this case except B0 all pump pulse are in low logic state. The inputs provided at the input ports of mrr1 and mrr 6. Since B0 is high mrr 11 will give low output. The signal from mrr1 is transferred to mrr4 and mrr5, in the same manner, the input of mrr6 is transferred to mrr10. In the presence of high pulse at B0, the combination of outputs from mrr4,5 and mrr10 will produce the signal high at drop port of mrr5 producing the result B>A.

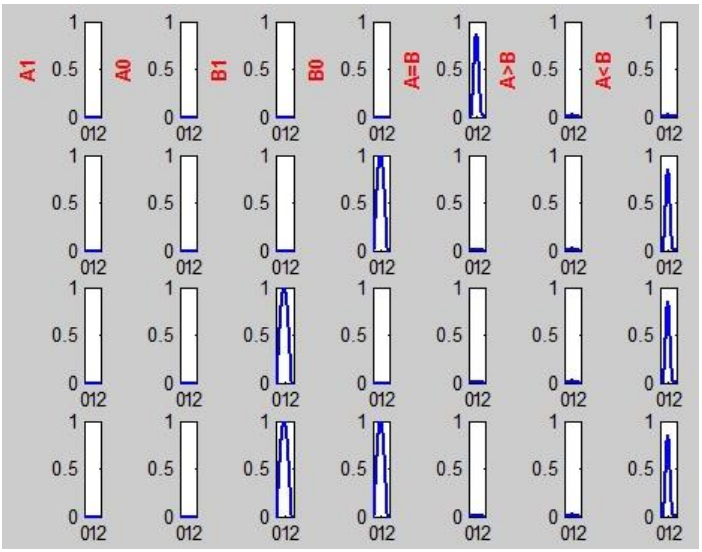

Fig. 6. Output of 2 bit comparator taking A=00 and varying B from 00 to 11 (color online)

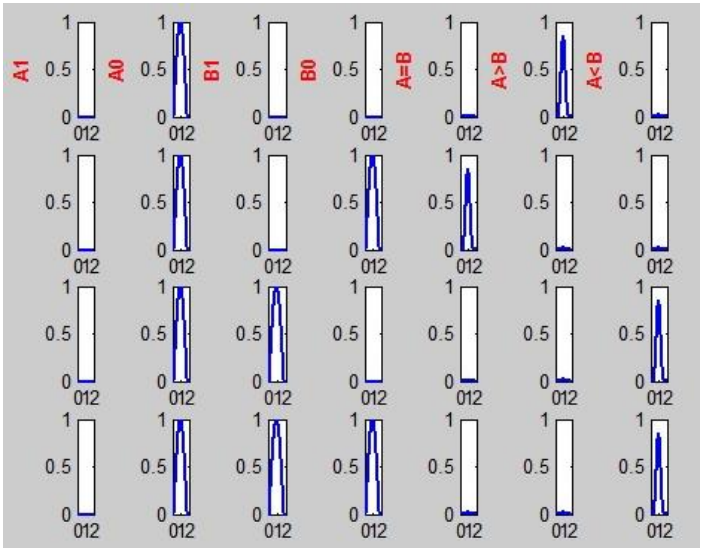

Fig. 7. Output of 2 bit comparator taking A=01 and varying B from 00 to 11 (color online)

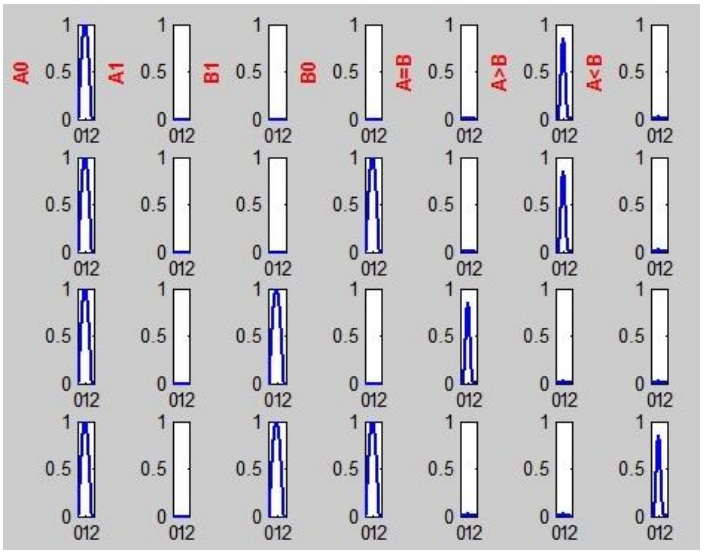

Fig. 8. Output of 2 bit comparator taking A=10 and varying B from 00 to 11 (color online)

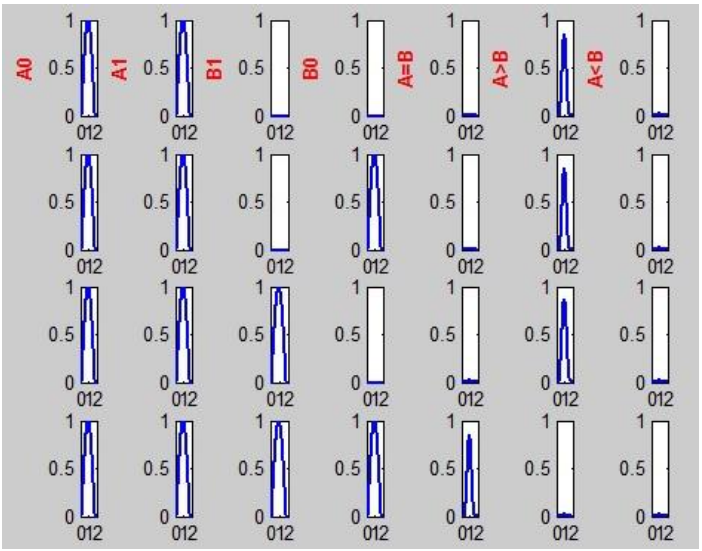

Fig. 9. Output of 2 bit comparator taking A=11 and varying B from 00 to 11 (color online)

Case 3 (A=00,B=10): This time the pump pulse B1 is logic high while rest are low. The signal is provided in the same manner at mrr1 and mrr6. The signal transferred from the drop port of mrr 10 to produce the output B>A.

Case 4 (A=00, B=11): In this situation when B1 and B0 is high. The through port of mrr 4 produce the signal high which gives B>A rest all the signal will be in logic low state.

Case 5(A=01, B=00): In this situation A0 is in logic high state and rest of the signal are in logic low state. The input from the input port of mrr 1 is transferred to the drop port of mrr 8 and input from mrr6 is transferred to drop port of mrr10, both the signal combined to produce the signal A>B high, all the other signals will be in the logic low state.

Case 6(A=01, B=01): In this case, A0 and B0 both are high producing input for mrr11 high. Similarly, the output of mrr 9 will also in the logic high state as A1 and B1 are logic low. Thus the pump signal of mrr11 is high and input is also high producing A=B.

Case 7(A=01, B=10): This time input from mrr 6 is transferred to drop port of mrr10 produce the signal B>A.

Case 8 (A=01, B=11): The pulses B0 and B1 are high therefore again the signal from the drop port of mrr10 produce B>A.

Case 9 (A=10, B=00): As A0 and B0 are same therefore the output will be decided as per A1 and B1. The signal from the input of mrr6 is transferred to the through port of mrr 10 to produce A>B.

Case10 (A=10, B=01): The input signal from mrr6 transferred to mrr10, the through port of mrr10 will produce A>B.

Case 11 (A=10, B=10): As both the signal A0 and B0 are logic low, therefore, the through output of mrr2 will be

high. Along with this through port of mrr9 is also high. Both signals are combined to produce high output at the through port of mrr11 which prove A=B.

Case 12 (A=10, B=11): In this case A1=B1, therefore, the through port of mrr4 will produce B>A.

Case 13(A=11, B=00): In this case, as A0 and A1 both are one, therefore, mrr7, 8 and mrr10 will produce A>B.

Case 14(A=11, B=01): In this case, the input from the mrr6 will be transferred to through port of mrr10 to produce A>B.

Case 15(A=11, B=10): The input from the mrr1 is transferred to mrr3. The mrr7 and mrr8 combined to produce A>B.

Case 16(A=11, B=11): As both the signal A0A1 and B0B1 are logic high therefore the through output of mrr2 and mrr9 will be high. Both signal are combined to produce high output at the through port of mrr11 which prove A=B.

7. Layout of J-K Flip-flop

The layout design for J-K flip-flop contains three microring resonator as shown in Fig. 10. The microring resonators are expected to resonant on wavelength ʎ. The incidence of optical pump pulse caused the change in the refractive index of the nonlinear material silicon nitride. The change in refractive index can be used to switch the input signal between through and drop ports of the microring resonator. In the design, the through port of mrr 1 is connected to input port of mrr 3, similarly the drop port of the mrr 2 is connected to add port of mrr 3. The drop port of mrr 3 will give the next state output. We have assumed the clock signal to be high.

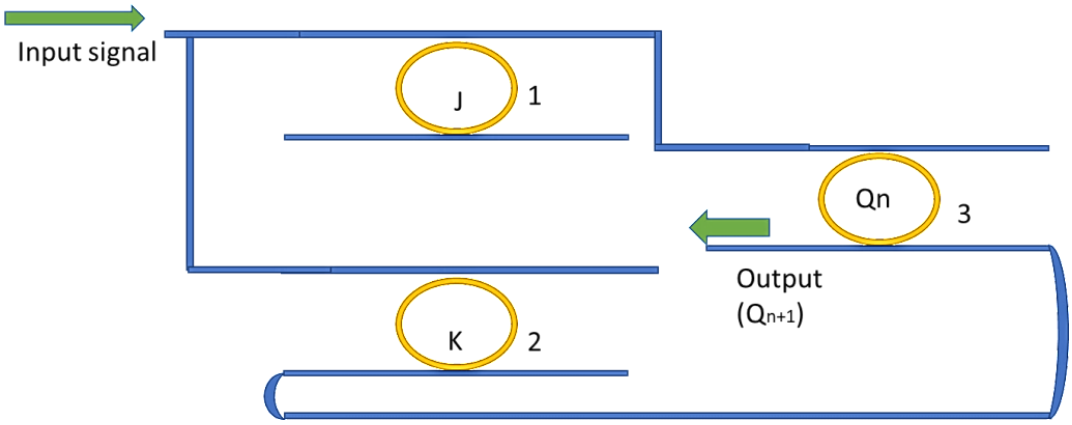

Fig. 10. Layout of J-K flip-flop

Table 2. J-K Flip-flop

Present state	J	K	Next state(Qn+1)
Q_n	0	0	$\mathbf{Q_n}$
X	0	1	0
X	1	0	1
Q_n	1	1	$\overline{Qn}$

8. Design and simulation

The simulation results of J-K flip-flop is shown in Fig. 11. The flip-flop is designed using Si3N4 based microring resonator. The working of J-K flip-flop can be compared with the truth table of J-K flip-flop as shown in Table 2. Assuming the previous state of the flip-flop is Qn the detailed functioning of the circuit can be explained as below

Case1 (J=0, K=0): When both J and K pump pulses are in off state. Both mrr1 and mrr2 are in on-resonance state, therefore the input is transferred to the add port of mrr 3 and whatever is the value of pump pulse Qn the drop port will give that output.

Case 2 (J=0, K=1): In this case when J pulse is off then mrr 1 will be on –resonance while K is in off-resonance state. Therefore irrespective of the value of pump pulse Qn, the ouput at the drop port of mrr 3 will be logic low.

Case 3(J=1, K=0): In this state, mrr1 will be off-resonance and mrr 2 will be on resonance therefore both the inputs of mrr 3 will be logic high and it results in high output at drop port of mrr 3 irrespective of value of pump pulse Qn.

Case 4 (J=1, K=1): As both, the pump pulses are logic high, therefore both the resonators (mmr1 and mrr3) are in the off-resonance state. Therefore the signal is reached to input port of mrr 3 which gives high output at the drop port when pump pulse Qn is low and vice-versa and therefor toggled the previous state (Qn).

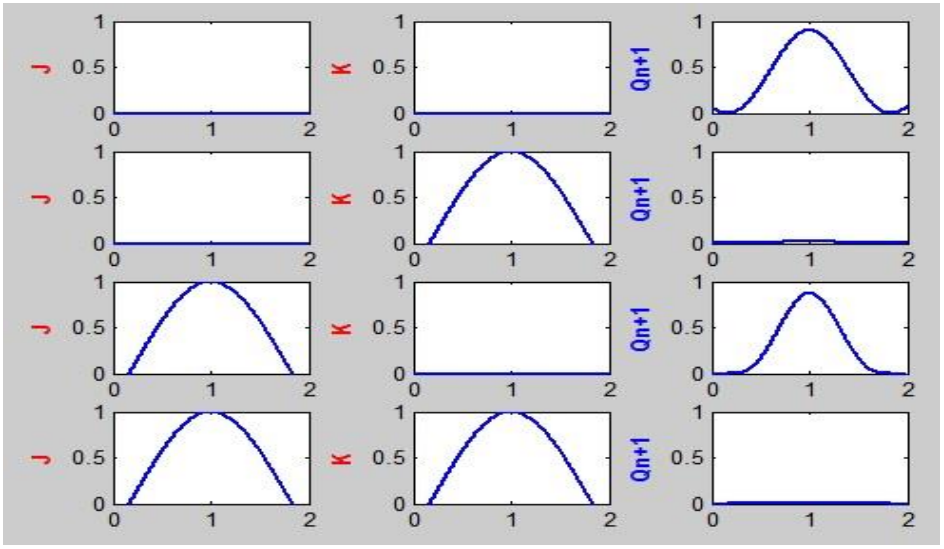

Fig. 11. The output of J-K flip-flop (color online)

9. Factors influencing the performance of microring resonator

The on-off ratio for the structure can be defined as the fraction of intensity in on resonance state to the without resonance state. The on-off ratio for the proposed structure is calculated using equation 15 and based on the graph obtained from simulation (shown below Fig. 12) and it comes around 24.9 dB which is better than previously proposed structure [13-14].

$$\text{On} - \text{off ratio} = \frac{\boldsymbol{T}_{\max(through\ port)}}{\boldsymbol{T}_{\min(drop\ port)}} \tag{15}$$

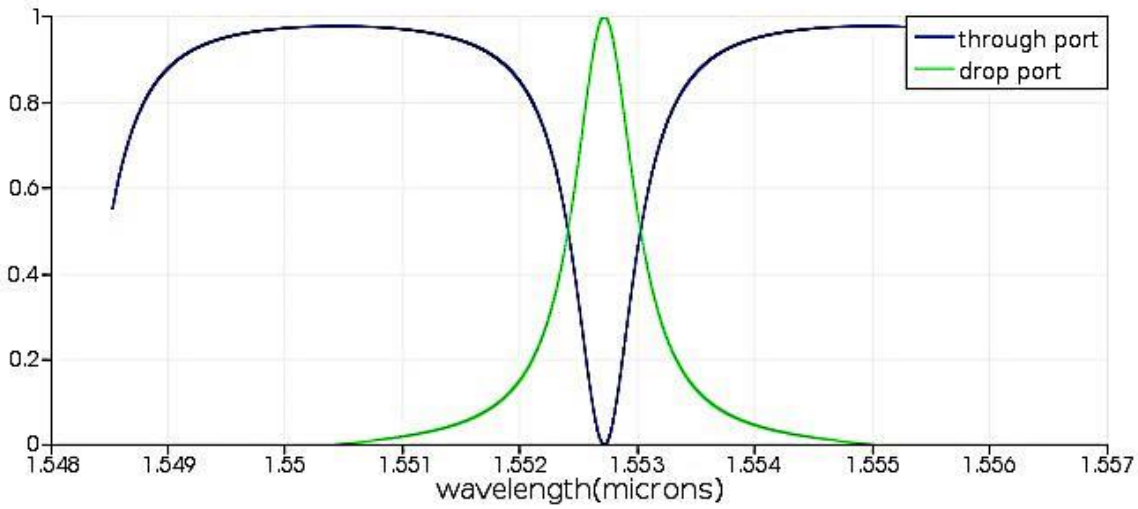

Fig. 12. Intensities at the output port

The extinction ratio (ER) is also calculated for our proposed structure as performance parameter, it can be given as the ratio of the minimum intensity of output signal for logical one (P_{min1}) to the maximum value of output intensity for logical zero (P_{max0}). Mathematically it can be given as shown below, for our structure its value is 20.29 dB which is also better than previous designs [13-14] as shown in Table 3. The contrast ratio (CR) achieved from the simulation is 19.54 dB. The value for amplitude modulation (AM) is calculated as 0.37 dB as per the equation 18.

$$\text{ER} = 10\log\frac{\text{P(min)}_1}{\text{P(max)}_0} \tag{16}$$

$$\text{CR} = 10\log\frac{\text{P(mean)}_1}{\text{P(mean)}_0} \tag{17}$$

$$AM = 10\log\frac{P(max)_1}{P(min)_1} \quad (18)$$

Some other important performance parameters for the presented configuration of ring resonator are finesse and quality factor. The finesse is the ratio of free spectral range to the FWHM (full width half maximum). The physical meaning of these two factors tells us about the number of round trips made by the optical energy inside the ring before getting lost due to losses. Mathematically quality factor and finesse can be denoted by

$$\text{Quality factor} = \frac{\text{resonant wavelength}(\Lambda)}{\text{FWHM}} \quad (19)$$

$$\text{Finesse} = \frac{FSR}{FWHM} \quad (20)$$

$$\text{FSR} = \frac{\lambda^2}{L.n} \quad (21)$$

The FWHM for the resonant structure is calculated as 0.20 nm. Accordingly, the calculated value of the quality factor for our structure is 7750. The FSR can be calculated in terms of wavelength as given in equation 21. The calculated value of FSR is 8 nm and as per FSR the value finesse is 40. We have used the optimum value of coupling coefficient to obtain the various figures of merit for the proposed design.as shown in Fig. 13.

Table 3. Comparison with the previous work

S.N	Parameters	Rakshit et.al. 2012-16	Kumar et.al. 2016	Proposed design
1	Material used	GaAs	GaAs	Si_3N_4
2	Coupling coefficients (α_1 and α_2)	0..25	0.25	0.35
3	Ring radius	7.048µm	7.048µm	20 µm
4	On-off ratio	20	20	25
5	Extinction ratio	12	12	40.29
6	Quality Factor	1400	1400	7750
7	Finesse	15	15	40

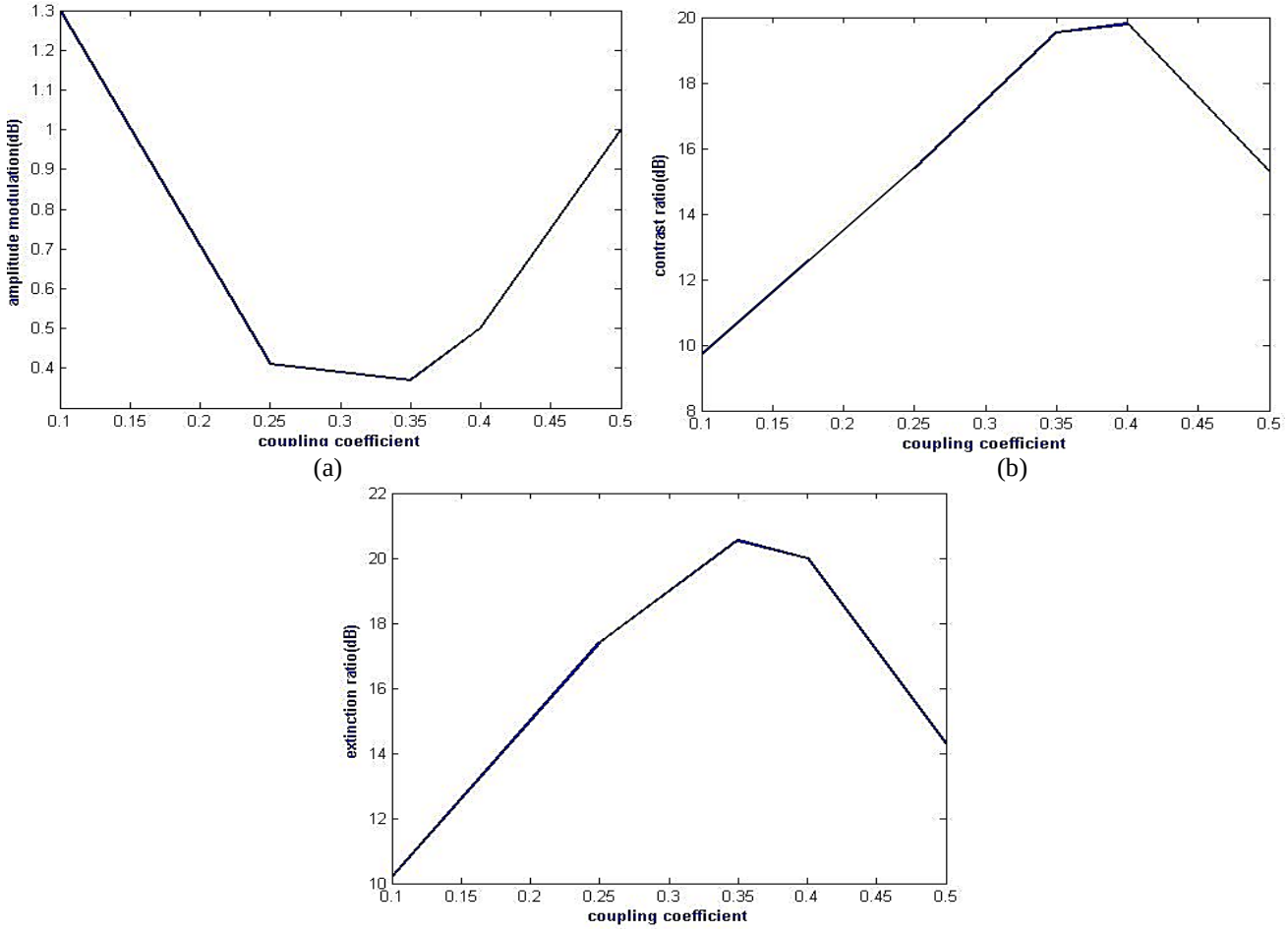

Fig. 13. (a) AM variation with coupling coefficient (b) CR variation with coupling coefficient (c) ER variation with coupling coefficient

10. Conclusion

We have described the numerical analysis of microring resonator especially for switching application. This article showed a novel magnitude comparator design and flip-flop using different combinations of the microring ring resonator. We have also calculated the various figures of merit (quality factor, on-off ratio, finesse, and contrast and extinction ratio) which influence the performance of ring resonators and proved the feasibility of the circuit. The ring resonator designed in this article simpler and can be utilized for many cascade application. The performance of cascaded microring resonator is satisfactory and showed a better result than previously reported work. The designed structure can be utilized for the construction of high order photonic integrated circuits. The optical logic circuits [18-19] are the future of logic processing machines and we are highly optimistic about the progress in this field in near future.

Acknowledgements

The authors are grateful to Department of ECE of Malaviya National Institute of Technology Jaipur, Department of TEQIP-III, MNIT, Jaipur and partner Malaysian and Vietnam Universities for providing the necessary support to carry out this work.

References

[1] Weijia Liu, Daquan Yang, Guansheng Shen, Huiping Tian, Yuefeng Ji, Opt. Laser Technol. **50**, 55 (2013).
[2] Sappasit Thongmeea, Preecha P. Yupapinb, 2nd International Science, Social-Science, Engineering and Energy Conference 2010 Engineering Science and Management Procedia Engineering **8**, 217 (2011).
[3] S. Soysouvanh, M. A. Jalil, I. S. Amiri, J. Ali, G. Singh, S. Mitatha, P. Yupapin, K. T. V. Grattan, M. Yoshida, Microsystem Technologies **24**(9), 3777 (2018).
[4] Dai Bo, Shimizu Satoshi, et al., IEEE Photonics Technology Letters **25**, 1 (2013).
[5] Ishizaka Yuhei, Kawaguchi Yuki, Koshiba Masanori, J. Lightwave Technol. **29**(18), 2836 (2011).
[6] A. Kumar, S. K. Raghuwanshi, Opt. Quantum Electron. **47**, 2117 (2015).
[7] S. K. Raghuwanshi, S. Kumar, Nan-Kuang Chen, Optics Communications **333**, 193 (2014).
[8] M. T. Hill, H. de Waardt, G. D. Khoe et al., IEEE J. Quantum Electron. **37**(3) 405 (2001).
[9] K. Luangxaysana, P. Phongsanam, S. Mitatha, M. Yoshida, N. Komine, P. P. Yupapin, Inf. Technol. J. **11**(10) 1470 (2012).
[10] Shaozhen Ma, Zhe Chen, Hongzhi Sun, Niloy K. Dutta, Opt. Express **18**, 6417 (2010).
[11] A. Godbole, P. P. Dali, V. Janyani, G. Singh, T. Tanabe, IEEE Journal of Selected Topics In Quantum Electronics **22**, 326 (2016).
[12] Godbole, P. P. Dali, G. Singh, T. Tanabe, International Conference on Computational Techniques in Information and Communication Technologies (ICCTICT), INSPEC Accession Number16143265, IEEE explore (2016).
[13] P. P. Dali, A. Godbole, S. Sahu, G. Singh, T. Tanabe, Asia Communications and Photonics Conference 2015, Hong Kong, OSA Technical Digest, ISBN: 978-1-943580-06, (2015).
[14] H. Kumar, V. Janyani, O. Buryy, S. Ubizskii, D. Sugak, G. Singh, Acta Physica Polonica A **133**(4), 997 (2018).
[15] J. K. Rakshit, J. N. Roy, T. Chattopadhyay, 5th International Conference on Computers and Devices for Communication 1 (2012).
[16] Ajay Kumar, Sanjeev Kumar Raghuwanshi, Optik **127**(20), 8751 (2016).
[17] J. K. Rakshit, T. Chattopadhyay, J. N. Roy, International Conference on Fiber Optics and Photonics, OSA paper WPo.29. (2012).
[18] A. Saharia, N. Mudgal, A. Agarwal. S. Sahu, S. Jain A. K. Ghunawat, G. Singh, A Comparative Study of Various All-Optical Logic Gates. In: Janyani V., Singh G., Tiwari M., d'Alessandro A. (eds.), Optical and Wireless Technologies. Lecture Notes in Electrical Engineering **546**, 429 (2019).
[19] A. Saharia, R. K. Maddila, J. Ali et al., Opt Quantum Electron. **51**, 224 (2019).

*Corresponding author: ankursaharia07@gmail.com